

Article

# Influence of NbC Addition on the Sintering Behaviour of Medium Carbon PM Steels

Doğan Özdemirler<sup>1</sup>, Süleyman Gündüz<sup>1,\*</sup> and Mehmet Akif Erden<sup>2</sup>

<sup>1</sup> Department of Manufacturing Engineering, Karabük University, Karabük 78050, Turkey; dozdemirler@hotmail.com

<sup>2</sup> Turkish Chambers and Stock Exchange Technical Science Vocational School, Karabük University, Karabük 78050, Turkey; makiferden@karabuk.edu.tr

\* Correspondence: sgunduz@karabuk.edu.tr; Tel.: +90-370-433-8200

Academic Editor: Laichang Zhang

Received: 9 February 2017; Accepted: 28 March 2017; Published: 1 April 2017

**Abstract:** In this work, the effects of NbC additions on the microstructure and mechanical properties were examined. In order to do this, NbC compounds were added into the Fe matrix at the weight percentage of 0.1–2 with individually to obtain powder mixture. The microstructure of the powder metallurgy (PM) steels were characterized by optic microscope, scanning electron microscope (SEM) and energy dispersive spectroscopy (EDS). Experimental results indicated that NbC alloyed steels can be produced by PM technology. An increase in strength was observed when the amount of NbC compounds increased for all PM steels. The precipitation of carbides and nitrides in these steels limits austenite grain growth and increases the precipitation hardening or clustering hardening that results in significant improvement in strength.

**Keywords:** powder metallurgy; PM steels; microstructure

## 1. Introduction

Microalloyed steels are materials that have outstanding specifications, such as high strength, high toughness, low ductile to brittle transition temperature, and resistance to corrosion with applications of various strengthening mechanisms and thermomechanical processes. Carbo-nitride which consists of elements like V, Nb, Al, and Ti, affects the mechanical properties of the steel when added below 0.2 wt % in terms of weight. However, it is necessary to calculate carefully the growth and resolution temperatures of the carbo-nitride. Otherwise, poorly-designed casting methods, rolling temperature, and cooling rate may lead to nonproduction or overgrowth of carbo-nitride. This will complicate the production of microalloyed steel with the casting method [1].

The carbon and manganese in microalloyed steels primarily contribute to solid solution strengthening. Additional, strength is obtained by precipitation of carbonitride particles which may occur at different stage during the manufacture and fabrication process of microalloyed steels [2,3]. The microalloying precipitates also prevent grain growth of the steels. In recent years, Nb–Ti alloy design has been used to produce hot rolled steels of yield strength 580–770 MPa characterized by good notch impact toughness and superior edge formability [4]. They were characterized by fine grain size (2–5  $\mu\text{m}$ ), narrow grain size distribution, inherently ductile behaviour, and microplasticity. Gao et al. [5] investigated the effect of lanthanum on the precipitation and dissolution of NbC in microalloyed steel using a combination method of thermo-mechanical experiment and the first-principle calculations. The experimental results showed that after deformation NbC precipitated more in La-free steel than in La-addition steel, and due to the relatively higher dissolution rate of NbC in La-addition steel, the Zener pinning effect decreased slightly faster, leading to a higher coarsening rate of austenite grain during isothermally heating at 1200 °C.

The advent of the technological era has brought the need for new materials to tackle everyday challenges of current materials for different applications. In the quest for new advanced materials, researchers have innovated various material systems. One of the most prominent material systems in the past few decades are metal matrix composites (MMC), where two or more constituents are used to fabricate a new material [6]. By formulating a composite, it is possible to use the unique advantages of different constituents in a complementary manner to suppress the limitations of each constituent [7]. Composite materials consist of two phases; one being a reinforcement as a transporter, and the other being a matrix which holds the reinforcement together in order to protect it from the outer effects. Countless combinations of matrix and reinforcement elements have been experimented since 1950 [1].

The incorporation of reinforcements into metal matrices significantly improves the hardness, tensile strength, elastic modulus, and other mechanical properties. Few other properties, such as thermal conductivity (TC), coefficient of thermal expansion (CTE), coefficient of friction, wear resistance, corrosion, and fatigue resistance, can also be tailored according to application requirements in metal matrix composites [8]. The use of different matrix and reinforcement elements have led to the development of various methods in the production of metal matrix composites (MMC). Production methods of the MMC are classified according to the liquid, solid, or gas phases of the matrix during production [9,10].

Many studies can be given as examples for the production of metal matrix composites. For example, Wang et al. [11] produced Fe matrix composites (Fe—50 wt % V, Fe—70 wt % Cr, Fe—50 wt % Mo) reinforced by (Ti,V)C in their work. Small (Ti,V)C particles are homogeneously dispersed in the Fe matrix. In addition, the authors found that the (Ti,V)C lattice parameter decreased with increasing V/Ti atomic ratio and morphology changed irregularly into a spherical shape. Hui et al. [12] investigated the high-temperature creep behaviour of Fe—Cr—Ni matrix composites containing 5–10 wt % and 16 wt % TiC particles at different temperatures (700–950 °C) and stresses (40–160 MPa). They observed that the creep deformation rates of composites decreased but the creep activation energy, initial stress, and creep life increased significantly due to the increase in the volume fraction of TiC particles. Wang et al. [13] have also investigated carbo-nitrides formed in Fe—(Ti,V)C composites. In their work, V/Ti-doped Fe—(Ti,V)C composites were produced by the powder metallurgy method in various atomic amounts. The experimental results show that (Ti,V)C particles are homogeneously dispersed in the Fe matrix and exhibit fine-grained structure which increased the strength of the composite materials.

It is observed during the literature research that composite component with Fe matrix is produced with the powder metallurgy method. However; it is also observed that the production of microalloyed steel with powder metallurgy is quite limited. The most important factor which separates microalloyed steel production and composite production is that weight ratios of the alloy elements added into the steel are different. This ratio is much higher in composite materials (1, 5, 10 and 50 wt %) while in microalloyed steel, it is 0.1–0.2 wt % maximum excluding Mn. Containing carbo-nitride particles at high volume fraction, composite materials with Fe matrix are prevalently utilised especially to improve the mechanical properties of steels. Surface quality of the composite materials, which are produced with the powder metallurgy method, is quite good and their dimensions are precise. Second-phase particles can be mixed in at a high ratio [9–13].

In this work, microalloyed and composite powder metallurgy (PM) steels were produced with the powder metallurgy method by adding NbC into Fe matrix at different ratios. The produced powder was pressed at 700 MPa in the molds as tensile test samples and alloyed PM steels were produced by sintering at 1400 °C in a tube-shaped atmosphere controlled furnace. The mechanical properties of produced PM steels were determined and the microstructure was investigated under sintered conditions to assess the role of precipitation strengthening and grain refinement.

## 2. Materials and Experimental Techniques

Powders for the production of alloyed PM steels were supplied by different companies. The specifications of these powders and scanning electron microscope (SEM) images of them are demonstrated in Table 1 and Figure 1, respectively.

**Table 1.** Powders used in experimental study and their properties.

Elemental Powders	Powder Size ( $\mu\text{m}$ )	Purity Value (%)	Supplied Company
Iron (Fe)	<150	99.9	Sintek (Istanbul, Turkey)
Carbon (C)	10–20	96.5	Sintek (Istanbul, Turkey)
Niobium Carbide (NbC)	$\leq 5$	97	Aldrich (Istanbul, Turkey)

As can be seen in Figure 1a, Fe powders used as matrix are generally in irregular form. C and NbC powders used as reinforcement elements generally have sharp corners and irregular geometry, as seen in Figure 1b,c.

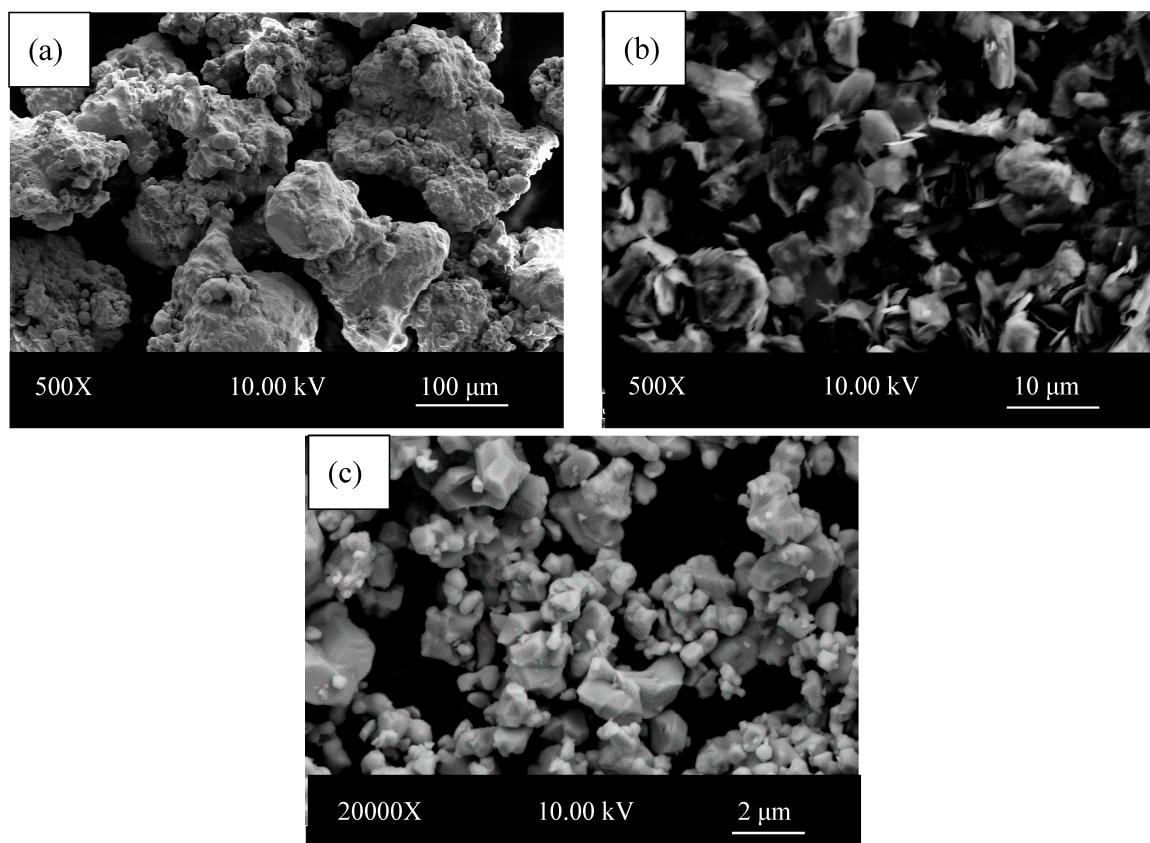


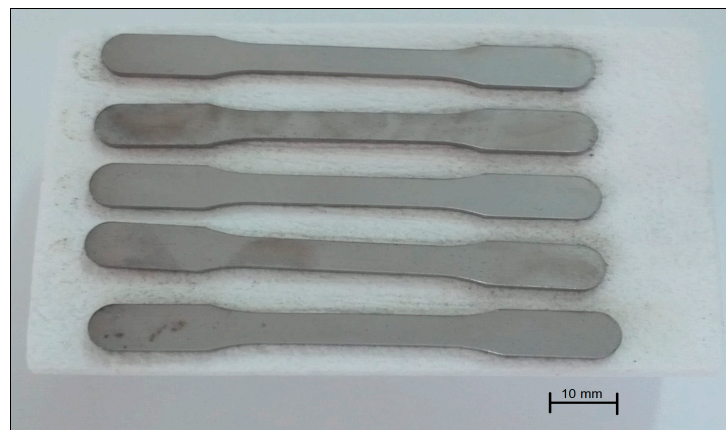
**Figure 1.** Scanning electron micrographs of Fe, C, and NbC powders (a) Fe  $\leq 150 \mu\text{m}$ ; (b) C 10–20  $\mu\text{m}$ ; and (c) NbC  $< 5 \mu\text{m}$ .

Before the mixing process, powders were weighed with a RADWAG AS-60-220 C/2 brand precision scale at 0.0001 g precision at the different ratios. The chemical composition of the powders are given in Table 2.

**Table 2.** Chemical composition of alloyed powder metallurgy (PM) steels.

Alloy	C (wt %)	NbC (wt %)	Fe (wt %)
Fe-0.3C	0.3	-	Rest
Fe-0.3C-0.1NbC	0.3	0.1	Rest
Fe-0.3C-0.2NbC	0.3	0.2	Rest
Fe-0.3C-0.5NbC	0.3	0.5	Rest
Fe-0.3C-1NbC	0.3	1	Rest
Fe-0.3C-2NbC	0.3	2	Rest

Weighed powders were mixed for 1 h without ball with a Turbula brand and three-axis mixer (Willy A. Bachofen AG, Muttenz, Switzerland). This mixture powders were unidirectionally pressed at 700 MPa in the form of tensile sample with 96 ton pressure capacity Hidroliksan brand device (Hidroliksan, Konya, Turkey) at room temperature. As can be seen in Figure 2, tensile samples were prepared according to the standards of ASTM (E8M) powder metal material.

**Figure 2.** Produced tensile test specimens.

In the experiment, PM steels were produced in six different chemical composition Fe-C, Fe-C-0.1 wt % NbC, Fe-C-0.2 wt % NbC, Fe-C-0.5 wt % NbC, Fe-C-1 wt % NbC and Fe-C-2 wt % NbC. Three tensile samples were produced for each PM steels and a total of 18 tensile samples were produced for 6 PM steels. Tensile samples were sintered at 1400 °C. Sintering process started by heating the samples up to sintering temperature with 5 °C/min speed. All samples were kept at 350 °C for 30 min in order to vaporize zinc stearate. When the temperature reached the sintering level, the samples were kept at this temperature for 1 h and then cooled up to room temperature with 5 °C/min speed.

Hardness measurement and tensile tests were applied for both unalloyed and alloyed PM steels. Hardness measurements (MCT-W, Shimadzu, Tokyo, Japan) were carried out by applying HV<sub>0.5</sub> (500 g) load. Five hardness measurements were obtained from each sample and the average of these was accepted as sample hardness value. Sintered tensile samples were tested by applying tensile force at 1 mm/min tensile speed. Stress-strain diagrams were obtained after each test. Based on these diagrams, yield strength (0.2%), tensile strength, and elongation (%) values of the samples were calculated.

Microstructure examinations were carried out with Nikon Epiphot 200 optical microscope (Melville, NY, USA) which has 50–1000× zooming capability. Different images were captured at different scales from different parts of each sample and attention was paid that these images represent the whole microstructure. Additionally, SEM (Carl Zeiss SMT GmbH, Oberkochen, Germany) and energy dispersive spectroscopy (EDS) (Carl Zeiss SMT GmbH, Oberkochen, Germany) analyses were carried out in order to determine the dimensions and types of the precipitate particles.

### 3. Results and Discussion

The microstructure images of the unalloyed and NbC-added PM steels sintered at 1400 °C are given in Figure 3.

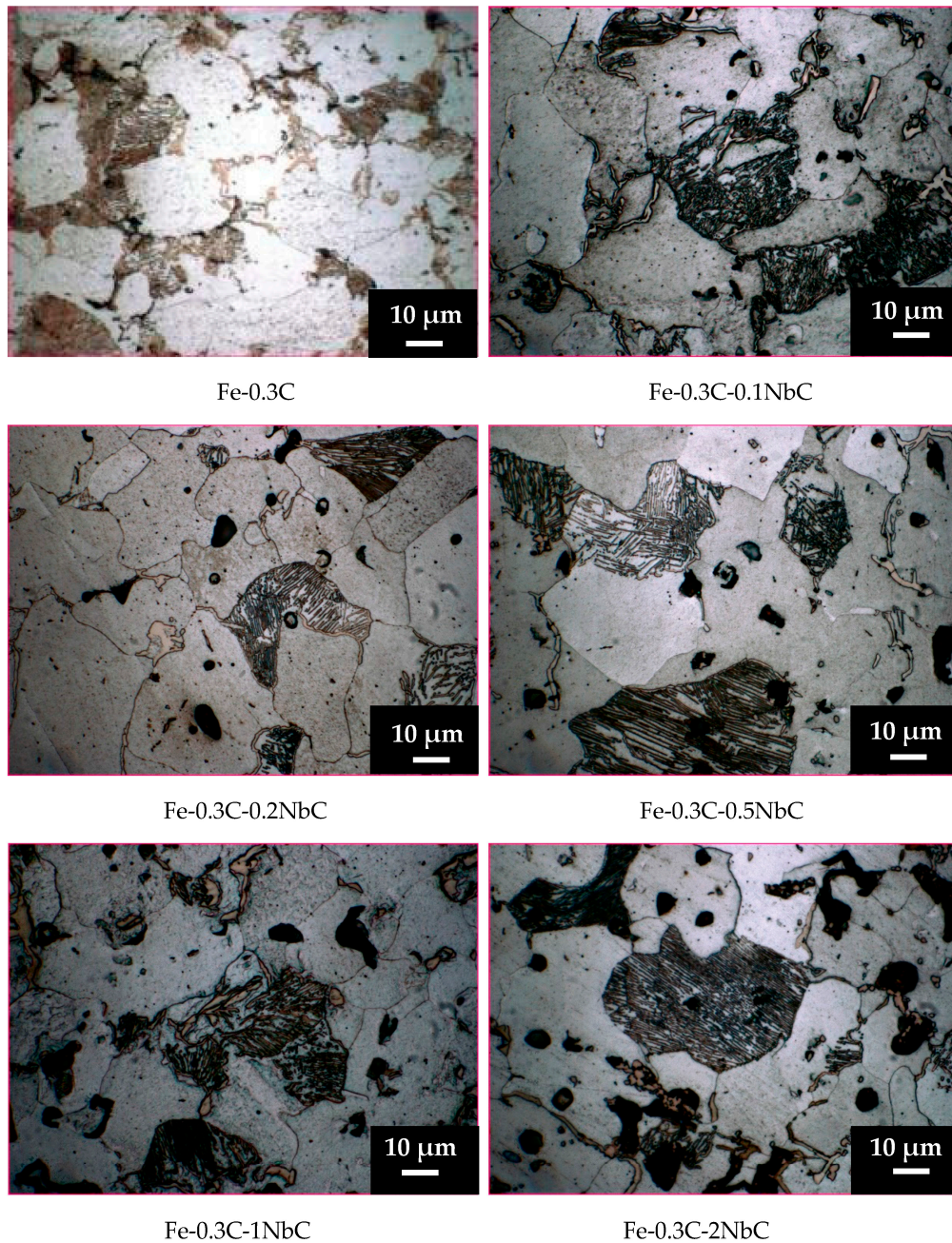


**Figure 3.** Microstructures of unalloyed PM steel and alloyed PM steels with different NbC contents sintered at 1400 °C for 1 h.

As can be seen, the microstructure of unalloyed and NbC-added PM steels consisted of ferrite and pearlite structures with different grain sizes. It is understood from the microstructure images that unalloyed PM steel, which was sintered at 1400 °C, has a larger grain size than NbC-added PM steels. For example, when the average grain size of the unalloyed PM steel is 33.6 μm, the average grain size was calculated 32.3, 31.4, 31.8, 32.1 and 33.3 μm with the amount of the NbC increases to 0.1, 0.2, 0.5, 1 and 2 wt %, respectively. Additionally, when the microstructure images are examined,

partially uncovered pores were observed on the grain boundaries. It is expressed in the literature that although porosity affects the toughness negatively, tiny and spherical pores do not decrease the strength [14]. Generally the mechanical properties of PM steels does not only be depends on the presence of pores but also mechanical behaviour of matrix and alloying elements have large impact on the final properties of the PM steels. Historically, it was wrongly assumed that the matrix's only role was to hold alloying elements or reinforcements in place. However, the importance of the matrix and its influence on the overall properties has been well established by researchers over the course of intensive investigations. Along with the properties of the alloying element or reinforcement, it is also very important to understand the interaction between the matrix and the alloying elements or the reinforcement. The interphase or the region between the matrix and the alloying elements or reinforcement actually plays a significant role in stress transfer between the matrix and the alloying element or the reinforcement. If the bonding between the two is weak; which can occur due to wettability issues or lack of interaction in between, the final material will have poor mechanical properties [8]. There are several studies on wettability of carbonaceous materials in aluminum-based composites. It is reported that various parameters, such as prior metallurgical history of the matrix, composition of the starting materials, processing temperature, and time have an effect on wettability of the carbon by molten aluminum and other metallic matrices [15].

Table 3 shows the relative density (%), porosity (%), ferrite (%), pearlite (%), and average mean linear intercept grain size of the unalloyed and NbC-added PM steels. It is seen in Table 3 that the relative density of the PM steels is generally about 94%. After sintering, there is, naturally, an increase in density. During the sintering process, the density of the PM steels increases by ensuring that the powder particles are connected to each other at a certain temperature and time. As a result of this, the PM steels gains a more homogeneous structure [16–18].

**Table 3.** Relative density (%), porosity (%), ferrite (%), pearlite (%), and mean linear intercept grain sizes of unalloyed PM steel and alloyed PM steels sintered at 1400 °C for 1 h.

Alloy	Relative Density (%)	Porosity (%)	Ferrite (%)	Pearlite (%)	Grain Size (µm)
Fe-0.3C	94.4	5.6	77.3	22.7	33.6
Fe-0.3C-0.1NbC	94.3	5.7	69.3	30.7	32.3
Fe-0.3C-0.2NbC	94.6	5.4	68.7	31.3	31.4
Fe-0.3C-0.5NbC	94.2	5.8	67	33	31.8
Fe-0.3C-1NbC	93.7	6.3	65	35	32.1
Fe-0.3C-2NbC	95.4	4.6	63	37	33.3

Additionally, as can be seen in Figure 3 and Table 3, the average grain size decreases when the NbC ratio increases up to 0.2% by weight. This occurs when NbC, NbN, and NbC(N) precipitates, which formed during sintering process, prevent growth of the austenite grains [19].

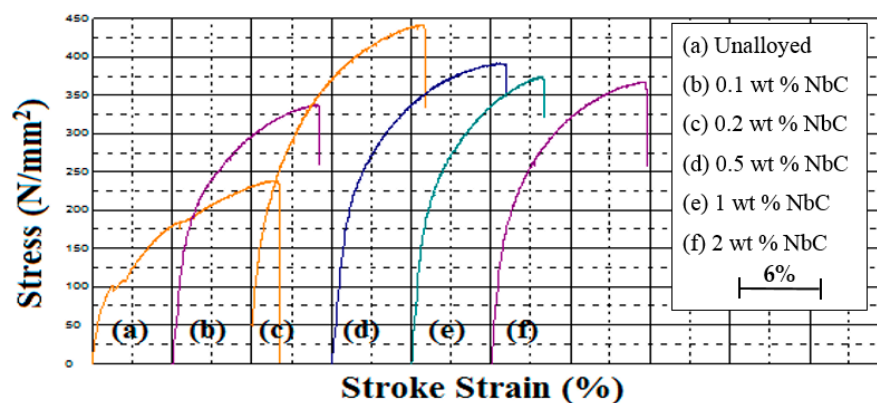
One of the most significant specifications of the alloy elements is that they prevent the grain growth by generating carbide and nitride during the austenitizing or sintering processes. The fact that small precipitates occur during austenitizing prevent austenite grain growth and lead to development of small ferrite grains in the course of cooling [20–22]. It was observed that the average grain size increased slightly with the NbC ratio increasing from 0.2% to 2% by weight. The fact that large NbC precipitates occur at the grain boundary can be considered as a reason for this increase [11,12]. Accumulation of large precipitates cannot prevent grain growth sufficiently.

Table 4 demonstrates the yield strength, tensile strength, elongation (%), and hardness values while Figure 4 shows the stress-strain diagrams of sintered PM steels. As can be seen in Figure 4 and Table 4, yield strength, tensile strength, and hardness values increase when NbC ratio increases to 0.2% in terms of weight, however elongation (%) values do not show any change. The carbides, nitrides, and carbo-nitride precipitates formed by Nb prevent the recrystallization and growth of the austenite, thereby ensuring that the materials have small grains. The fact that there are more grain boundaries in the small-grained structure, and these grain boundaries stop the dislocation

movement increases the strength. A decrease in the grain size increases the elongation (%) of the PM steels. Alongside this, the developed precipitates contribute to increase of the yield strength, tensile strength and hardness values with different strengthening mechanisms, such as precipitation hardening, dispersion hardening, and clustering hardening [23–25].

**Table 4.** Mechanical properties of PM steels sintered at 1400 °C for 1 h.

Alloy	Yield Strength (MPa)	Ultimate Tensile Strength (MPa)	Elongation (%)	Hardness (HV <sub>0.5</sub> )
Fe–0.3C	100	240	14	65
Fe–0.3C–0.1NbC	185	339	11	99
Fe–0.3C–0.2NbC	235	443	13	139
Fe–0.3C–0.5NbC	215	393	13	129
Fe–0.3C–1NbC	205	376	12	121
Fe–0.3C–2NbC	200	369	12	115

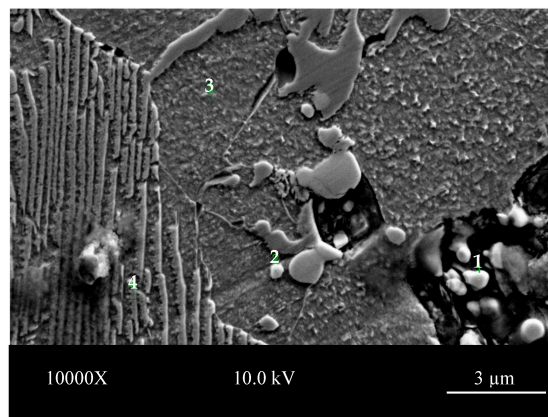


**Figure 4.** Variation of stress–strain curves of the unalloyed PM steel and alloyed PM steels with different NbC contents sintered at 1400 °C for 1 h.

There is a decrease in the yield strength, tensile strength, and hardness values when the NbC ratio increases from 0.2% to 2% in terms of weight. Generally, compared to unalloyed PM steel, an increase in the strength values of all the NbC-added PM steels were observed. This change in strength values is a consequence of the formation of NbC(N) precipitates and their dispersion in the matrix in different sizes [24]. During the sintering at 1400 °C or cooling after sintering, the formed precipitates increase the yield strength, tensile strength, and hardness values of the PM steels to which NbC was added. However, if the amount of NbC is more than 0.2% by weight, it reduces the strength. This indicates that an excessive amount of coarse NbC precipitates are present both in the grain boundary and inside the grain and it leads to the lower strength [16–18]. Another reason for the low strength of the PM steel which contains 2 wt % NbC is that density is also low in this steel. The specifications like strength, ductility, and conductivity depend on the density; in other words, the porosity and structure of the pores [17].

SEM image and EDS point analysis of the PM steels which have 2% NbC by weight can be seen in Figure 5. SEM image of PM steels with 2% NbC by weight indicated the presence of precipitates with different sizes. Additionally, results of the EDS point analysis show that these precipitates are NbC, because they contain Nb and carbon elements. SEM and EDS analysis also showed the presence of NbC(N) precipitates in steel. These precipitates prevented austenite grain growth and re-crystallisation and increased the hardness of the PM steels with precipitation hardening [26].

The effect of the alloy elements in the solid solution on the re-crystallisation of austenite is very weak. The inhibition of the grain boundary movement by precipitated particles is much more effective than dissolved atoms [27]. Microstructure, SEM, and EDS analysis indicated that Nb is in the solution and in the form of precipitate particles.



Spectrum				
Atomic Percent (%)	C	N	Nb	Fe
1	49.82	1.12	42.84	3.48
2	52.47	2.68	31.15	8.51
3	9.83	0.97	0.00	86.71
4	15.71	0.91	0.00	81.19

**Figure 5.** SEM micrograph of PM steels with 2 wt % NbC content sintered at 1400 °C for 1 h. And corresponding EDS of the indicated points.

Moreover, Figure 6 shows the results of the EDS line analysis from matrix and precipitates of the PM steels containing 0.2% NbC and 2% NbC by weight, which is sintered at 1400 °C. When the EDS line results of 0.2 and 2 wt % NbC-added steel were examined, there seems to be a difference between the type and amount of the element throughout the line which cuts the matrix and the precipitate. It is observed that the matrix phase is rich in iron, but the precipitate is rich in Nb.

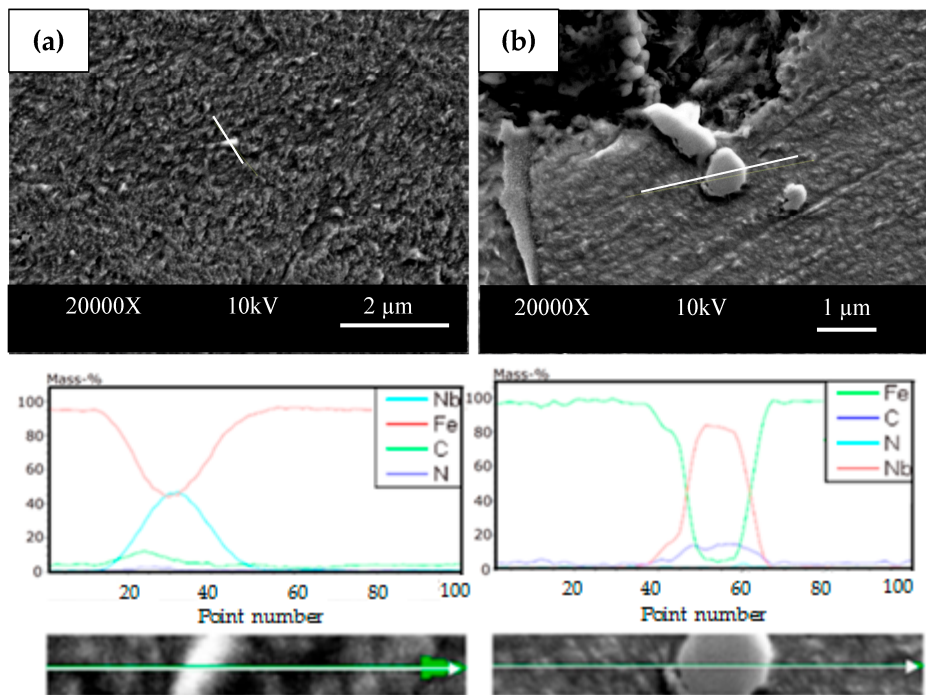


**Figure 6.** SEM micrographs and EDS line scan of the indicated particles for 0.2 wt % NbC-added steel (a) and 2 wt % NbC added steel (b) sintered at 1400 °C for 1 h.

After the tensile test, the fracture surfaces of alloyed PM steels containing 0.2 and 2 wt % NbC and sintered at 1400 °C were analysed at 80 $\times$ , 1000 $\times$  and 5000 $\times$ . Figure 7a,b show the fractographs of the 0.2 wt % NbC and 2 wt % NbC-added steels and the results of the EDS point analysis obtained from the fracture surface. It is seen in the same figure that dimples and cleavage facets are together on the fracture surface of the NbC-added PM steel. For this reason, it can be said that the structure is partially ductile and partially brittle.

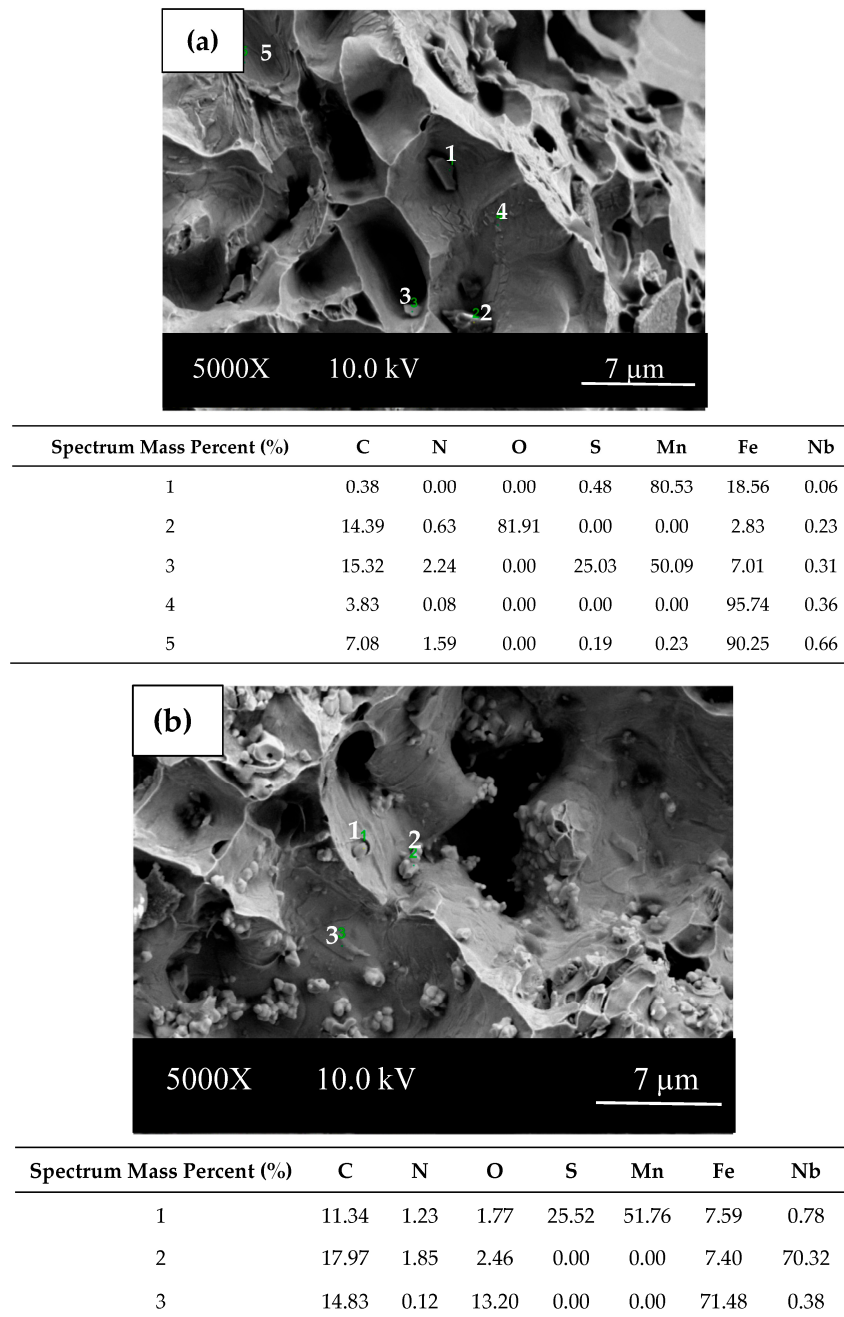


**Figure 7.** Fracture surfaces and EDS results from indicated points of PM steels sintered at 1400 °C for 1 h; (a) 0.2 wt % NbC and (b) 2 wt % NbC.

Moreover, large voids were observed in alloyed steel samples which contain 0.2 and 2 wt % NbC sintered at 1400 °C. These voids are indicative of the removal of NbC(N) particulates through pulling off under heavy tensile loading conditions. Shanmugasundaram and Chandramouli [28] found that

these kinds of voids occurred on the fracture surfaces of the powder metallurgy steel, which contains Cr, Ni and Mo. This was attributed to the formation of carbides and carbide breaking off from the surface during heavy deformation.

EDS point analysis, which is taken from the fracture surface of the 1400 °C sintered and 0.2 and 2 wt % NbC-added steels, indicates that the precipitates rich in Nb are existent in steel. This situation shows that the precipitates such as NbC(N) occurred in the steel during sintering or cooling after sintering process. These precipitates affect the fracture surface morphology of the alloyed PM steel.

#### 4. Conclusions

Alloyed PM steels with six different volume fractions (0, 0.1, 0.2, 0.5, 1 and 2 wt % NbC) were produced by cold pressing, followed by sintering at 1400 °C in an argon atmosphere. The results listed below are obtained from this study.

1. There is an increase in the yield strength, tensile strength, and hardness values of the PM steel when the amount of NbC increases to 0.2% in terms of weight. This is a result of the formation of the precipitates such as Nb(N), NbC, or NbC(N) during the sintering or cooling after the sintering process.
2. The strength of the steels decreases when the amount of NbC is more than 0.2% by weight. This indicates that excessive amount of coarse NbC precipitates are present both in the grain boundary and inside the grain and it leads to the lower strength.
3. SEM and EDS analyses show that NbC, NbN, and NbCN occurred in the NbC-added PM steels. These different precipitates formed affect the mechanical properties of the PM steels.
4. When fracture surfaces of PM steels are examined, all of the surfaces appeared partially ductile (dimple structure) and partially brittle (cleavage structure), giving a mixed fracture. This is in agreement with the elongation (%) values.

**Acknowledgments:** This work was supported by Scientific Research Projects Coordination Unit of Karabük University (Karabük, Turkey). Project Number: KBÜ-BAP-15/2-YL-016.

**Author Contributions:** Mehmet Akif Erden and Doğan Özdemirler designed the experiments, performed the experiments, analysed the data and wrote the paper. Süleyman Gündüz directed the research and contributed to the discussion and interpretation of the results.

**Conflicts of Interest:** The authors declare no conflict of interest.

#### References

1. Ateş, S.; Uzun, İ.; Çelik, V. The effect of infiltration temperature on the thermal conductivity of SiC/Al 2014 composite produced by Pressured Infiltration Method. In Proceedings of the IATS'11, Elazığ, Turkey, 16–18 May 2011; pp. 16–18.
2. Thridandapani, R.R.; Misra, R.D.K.; Mannering, T.; Panda, D.; Jansto, S. The application of stereological analysis in understanding differences in toughness of V and Nb microalloyed steels of similar yield strength. *Mater. Sci. Eng. A* **2006**, *442*, 285–291. [[CrossRef](#)]
3. Gündüz, S.; Cochrane, R.C. Influence of cooling rate and tempering on precipitation and hardness of vanadium microalloyed steel. *Mater. Des.* **2005**, *26*, 486–492. [[CrossRef](#)]
4. Misra, R.D.K.; Tenneti, K.K.; Weatherly, G.C.; Tither, G. Microstructure and texture of hot-rolled Cb–Ti and V–Cb microalloyed steels with differences in formability and toughness. *Metall. Trans. A* **2003**, *34*, 2341–2351. [[CrossRef](#)]
5. Gao, X.; Ren, H.; Wang, H.; Chen, S. Effect of lanthanum on the precipitation and dissolution of NbC in microalloyed steels. *Mater. Sci. Eng. A* **2017**, *683*, 116–122. [[CrossRef](#)]
6. Sharma, P.; Khanduja, D.; Sharma, S. Tribological and mechanical behavior of particulate aluminum matrix composites. *J. Reinf. Plast Compos.* **2014**, *33*, 2192–2202. [[CrossRef](#)]
7. Surappa, M.K. Aluminium matrix composites: Challenges and opportunities. *Sadhana* **2003**, *28*, 319–334. [[CrossRef](#)]

8. Shirvanimoghaddam, K.; Hamim, S.U.; Akbaric, M.K.; Fakhrhoseinia, S.M.; Khayyama, H.; Paksereshtd, A.H.; Ghasalid, E.; Zabete, M. Carbon fiber reinforced metal matrix composites: Fabrication processes and properties. *Composite Part A* **2017**, *92*, 70–96. [[CrossRef](#)]
9. Kalemtaş, A. An Overview of Metal Matrix Composites. *Putech Compos.* **2014**, *5*, 18–30.
10. Doğan, Ö.N.; Hawk, J.A.; Tylczak, J.H.; Wilson, R.D.; Govier, R.D. Wear of titanium carbide reinforced metal matrix composites. *Wear* **1999**, *225–229*, 758–796. [[CrossRef](#)]
11. Wang, J.; Wang, Y.; Ding, Y. Production of (Ti,V)C reinforced Fe matrix composites. *Mater. Sci. Eng. A* **2007**, *445–455*, 75–79.
12. Hui, X.D.; Yang, Y.S.; Wang, Z.F.; Yuan, G.Q.; Chen, X.C. High temperature creep behavior of in-situ TiC particulate reinforced Fe–Cr–Ni matrix composite. *Mater. Sci. Eng. A* **2007**, *282*, 187–192. [[CrossRef](#)]
13. Wang, J.; Wang, Y.; Ding, Y. Microstructure and wear-resistance of Fe–(Ti,V)C composite. *Mater. Des.* **2007**, *28*, 2207–2209. [[CrossRef](#)]
14. Saritas, S.; Causton, R.; James, B.; Lawley, A. Effect of Microstructural Inhomogeneities on the Fatigue Crack Growth Response of a Prealloyed and Two Hybrid P/M Steels. *Adv. Powder Metall. Part Mater.* **2002**, *5*, 112–117.
15. Eustathopoulos, N.; Joud, J.C.; Desre, P.; Hicter, J.M. The wetting of carbon by aluminium and aluminium alloys. *J. Mater. Sci.* **1974**, *9*, 1233–1242. [[CrossRef](#)]
16. Erden, M.A.; Gündüz, S.; Karabulut, H.; Türkmen, M. Effect of V Addition on the Microstructure and Mechanical Properties of Low Carbon Microalloyed Powder Metallurgy Steels. *Mater. Test.* **2016**, *58*, 433–437. [[CrossRef](#)]
17. Schade, C.; Murphy, T.; Lawley, A.; Doherty, R. Microstructure and mechanical properties of microalloyed PM steels. *Int. J. Powder Metall.* **2012**, *48*, 51–59.
18. Schade, C.; Murphy, T.; Lawley, A.; Doherty, R. Microstructure and mechanical properties of PM steels alloyed with silicon and vanadium. *Int. J. Powder Metall.* **2012**, *48*, 41–48.
19. Ollilainen, V.; Kasprzak, W.; Hollapa, L. The effect of silicon, vanadium and nitrogen on the microstructure and hardness of air cooled medium carbon low alloy steel. *J. Mater. Process. Technol.* **2003**, *134*, 405–412. [[CrossRef](#)]
20. Huo, X.; Mao, X.; Lv, S. Effect of annealing temperature on recrystallization behavior of cold rolled Ti-microalloyed steel. *J. Iron Steel Res. Int.* **2013**, *20*, 105–110. [[CrossRef](#)]
21. Bakkali, E.H.F.; Chenaouia, A.; Dkiouaka, R.; Elbakkalib, L.A.O.A. Characterization of deformation stability of medium carbon microalloyed steel during hot forging using phenomenological and continuum criteria. *J. Mater. Process. Technol.* **2008**, *1999*, 140–149.
22. Gladman, T. *The Physical Metallurgy of Microalloyed Steels*, 1st ed.; The Institute of Materials: London, UK, 1997.
23. Cuddy, L.C.; Raley, J.C. Austenite Grain Coarsening in Microalloyed Steels. *Metall. Mater. Trans. A* **1983**, *14*, 1989–1995. [[CrossRef](#)]
24. Llewellyn, D.T.; Hudd, R.C. *Steels: Metallurgy and Applications*, 3rd ed.; Reed Educational and Professional Publishing Ltd.: Oxford, UK, 1998; pp. 15–40.
25. Erden, M.A.; Gündüz, S.; Türkmen, M.; Karabulut, H. Microstructural characterization and mechanical properties of microalloyed powder metallurgy steels. *Mater. Sci. Eng. A* **2014**, *616*, 201–206. [[CrossRef](#)]
26. Kostyryzhev, A.G.; Al Shahrani, A.; Zhu, C.; Cairney, J.M.; Ringer, S.P.; Killmore, C.R.; Pereloma, E.V. Effect of niobium clustering and precipitation on strength of an NbTi-microalloyed ferritic steel. *Mater. Sci. Eng. A* **2014**, *607*, 226–235. [[CrossRef](#)]
27. Korczynsky, M. Microalloying and thermo-mechanical treatment. In Proceedings of the International Symposium on Microstructure and Properties of HSLA Steels, Pittsburgh, PA, USA, 3–5 November 1987; pp. 169–201.
28. Shanmugasundaram, D.; Chandramouli, R. Tensile and impact behaviour of sinter-forged Cr, Ni and Mo alloyed PM steels. *Mater. Des.* **2009**, *30*, 3444–3449. [[CrossRef](#)]

